Supporting Information

"POM-Lock" Nanozymes Serve As Chirality-Keyed Bacterial Membrane Disruptors And Wound Repair Agents For Chemodynamic Therapy

Ying Tao[a], Shuo Wang[a], Yue Meng[a], Zhengya Yue[a], Qingyao Meng[a], Xue Li[a], Tiedong Sun[a*]

a. College of Chemistry, Chemical Engineering and Resource Utilization, Northeast Forestry University, Harbin, 150040, PR China

Corresponding Author：

Prof. Tiedong Sun, E-mail: tiedongsun@nefu.edu.cn (Sun T)

This supplemental file includes:

1. Experimental Procedures

Materials: Sodium tungstate dihydrate ($Na_2WO_4 \cdot 2H_2O$, 99.5%), Potassium chloride (KCl, 99.5%), Zinc acetate dihydrate ($Zn(CH_3COO)_2 \cdot 2H_2O$, 99%), Copper sulfate ($CuSO_4$, 99%), Glacial acetic acid (CH_3COOH, 99%), D-Proline (D-Pro, 99%), L-Proline (L-Pro, 99%), Copper chloride dihydrate ($CuCl_2 \cdot 2H_2O$), 3,3',5,5'-tetramethylbenzidine (TMB, ≥99%), Methylene blue (MB, 70%), Terephthalic acid (TA, ≥99%), 5,5'-dithiobis (2-nitrobenzoic acid) (DTNB, 98%), Glutathione (GSH, 98%), 2,7-dichlorodihydrofluorescein diacetate (DCFH-DA, 98%), 3-(4,5-dimethylthiazole-2-yl)-2,5-diphenyltetrazolium bromide (MTT, 98%), Acridine orange (AO, ≥75%), 4,6-diamido-2-phenylindole (DAPI, 98%), Calcium yellow green pigment (AM, ≥96%), and Propidium iodide (PI, ≥98%). All products were purchased from Aladdin Reagent Company in Shanghai, China. The crystal violet staining solution was purchased from Shanghai Biyun Tian Biotechnology Co., LTD.

Synthesis of polyoxometalate nanozymes (POMs)

First, 36.3 g (110 mmol) of sodium tungstate dihydrate ($Na_2WO_4 \cdot 2H_2O$) was dissolved in 135 mL of deionized water, and then the pH of the solution was adjusted to 6.3 with glacial acetic acid. Subsequently, the mixture was heated to 80 degrees Celsius. Under the condition of continuous stirring, 2.2 g (10 mmol) of zinc acetate dihydrate ($Zn(CH_3COO)_2 \cdot 2H_2O$) was dissolved in 15 mL of water to prepare a solution. Add 20 mL of copper sulfate ($CuSO_4$) solution with a concentration of 0.5 mmol/mL drop by drop, and then add 15 g (201 mmol) of potassium chloride (KCl) to obtain the first batch of light blue precipitate. Subsequently, a blue-green crystalline product is obtained through recrystallization ($K_{10}(ZnW_{11}CuO_{34})$)[1].

Synthesis of D-polyoxometalate nanozyme (D-POMs)

D-proline (0.0576 g, 0.5 mmol) and copper chloride dihydrate ($CuCl_2 \cdot 2H_2O$, 0.0852 g, 0.5 mmol) were dissolved in 30 mL of water. Carefully adjust the pH value of the mixture to approximately 4.50 with 1 M dilute sodium hydroxide solution, and then stir for 2 h. Then, 30 mL of aqueous solution containing 0.7715 g (0.25 mmol) of the polyoxometalate nanozyme synthesized above was added, and the resulting solution was heated at 80℃ for 2 h. The filtrate was placed under environmental conditions for 1 month, and the green compound D-POM crystals were separated[2].

Synthesis of L-polyoxometalate nanozyme (L-POMs)

The synthesis of compound L-POM was performed as described above for the synthesis of compound D-POM, but L-proline was used as starting material[2].

Characterization of D/L-POM

In order to determine the morphology, structure and elemental composition of D/L-POM, scanning electron microscopy (SEM; JSM-7500F, Produced by Japan Electronics Corporation (JEOL)) and transmission electron microscopy analysis (TEM; Model JEM-2100, Japan Electronics Corporation (JEOL)). Particle size and surface charge of samples were detected by particle size analysis and Zeta potential measurement using Malvern Particle size Analyzer (model Zeta sizer Nano S90, Malvern Instruments LTD, UK). X-ray diffraction analysis (XRD; Rigaku, Japan), Fourier transform infrared spectroscopy (FTIR, Thermo Fisher Scientific) and X-ray photoelectron spectroscopy (XPS; Model PHI 5700 ESCA System, Physionics, USA) to analyze the composition and valence states of the samples. A circular dichroic spectrometer (model Chirascan VX; Produced by Applied Photophysics, UK) for chiral analysis of the samples.

Chemical kinetic performance analysis of D/L-POM

Determination of reactive oxygen species (ROS): The generation of ROS was verified by the methylene blue (MB) degradation method. Different concentrations of D/L-POM nanoenzyme solutions (10 μg/mL, 20 μg/mL, 30 μg/mL, 40 μg/mL and 50 μg/mL) were co-reacted with methylene blue and hydrogen peroxide respectively. The absorption spectrum of the solution was determined by a ultraviolet-visible absorption spectrometer, and the ROS generation capacity was measured by the intensity change at 664 nm. The ROS generation capacity was further detected by using 3,3',5,5'-tetramethylbenzidine (TMB). Different concentrations of D/L-POM nanoenzyme solutions (10 μg/mL, 20 μg/mL, 30 μg/mL, 40 μg/mL and 50 μg/mL) were co-reacted with TMB and hydrogen peroxide respectively. The absorption spectrum of the solution was determined by ultraviolet-visible spectroscopy, and the ROS production capacity was measured by the intensity change at 652 nm[3].

Determination of hydroxyl radicals (·OH): Terephthalic acid (TA) fluorescence detection method was used to verify the production of ·OH. Different concentrations of D/L-POM solution (100 μg/mL, 200 μg/mL, 300 μg/mL, 400 μg/mL, 500 μg/mL) were used to react with terephthalic acid. The amount of ·OH produced was verified by measuring the fluorescence intensity by a steady-state transient fluorescence spectrometer.

Electron paramagnetic resonance (ESR) spectroscopy was performed with the assistance of trapping agents to further analyze the type and generation of ROS. In brief, 5,5'-dimethyl-1-pyrroline-N-oxide (DMPO, Aladdin) was used to capture ·OH produced after incubation of the sample with H_2O_2 for a certain time[4].

Dynamic performance analysis: According to the catalytic mechanism of steady-state catalytic kinetics, the fitting curve conforms to the Michaelis equation (2-1)[5]:

$$V_0 = \frac{V_{max} \cdot [S]}{(K_m + [S])} \qquad (2\text{-}1)$$

Here, V_{max} represents the maximum reaction rate and [S] represents the substrate concentration. According to Equation (2-2), K_m and V_{max} of D-POM and L-POM catalyzed reaction were determined by Line weaver-Burk diagram[5]:

$$\frac{1}{V_0} = \frac{K_m}{V_{max}} \cdot \frac{1}{[S]} + \frac{1}{V_{max}} \qquad (2\text{-}2)$$

Determination of glutathione (GSH) degradation: 5,5'-dithiobbis (2-nitrobenzoic acid) (DTNB) was used as a probe to verify GSH content by chromogenic method. Different concentrations of D/L-POM nanoenzyme solutions (10 μg/mL, 20 μg/mL, 30 μg/mL, 40 μg/mL and 50 μg/mL) were used to react with GSH. The absorption spectrum of the solution was measured by UV-vis spectroscopy, and the peak at the UV absorption wavelength 412 nm was verified to analyze the degradation ability of GSH by nanoparticles with different concentrations[6].

Evaluation of *in vitro* antibacterial performance

Coated plate method: Escherichia coli (*E.coli*) and Staphylococcus aureus (*S.aureus*) were used as representative strains of Gram-negative and Gram-positive bacteria, respectively, to evaluate the antimicrobial properties of the samples. Typically, *E.coli* and *S.aureus* were co-cultured with phosphate buffer (PBS), POM, D-POM, and L-POM for 6 h, respectively. After these treatments, 20 μL of the suspension was removed from each well and then coated on LB AGAR plates. These

plates were incubated at 37℃ for 12 h to observe colonies. Bacterial survival (S%) was calculated using the following equation[7]:

$$S\% = C_{sam}/C_{con} \times 100\%$$

Among them, C_{sam} and C_{con} respectively represent the colony units of different samples and control groups (phosphate buffered saline, PBS).

***In vitro* time-kill assay evaluation:** The viable bacterial counts of *E. coli* and *S. aureus* following treatment with D/L-POM at various time intervals were determined via the plate counting method, and time–kill curves were generated.

Scanning electron microscope (SEM) was used for observation: Add 1 mL of *S.aureus* suspension and 1 mL of *E.coli* suspension (both with concentrations of 1×10^4 colony-forming units/ml) to 6-well plates containing slides, respectively. After incubation for 24 h, discard the culture medium and add different samples. Then, fix the sample with 4% paraformaldehyde for 1 h. Then, the samples were dehydrated using gradient ethanol solutions (10%, 30%, 50%, 70%, 90% and 100% ethanol). Subsequently, gold was sputtered onto the slide for observation under a scanning electron microscope[8].

Live-dead staining assay: The *S.aureus* suspension (1 mL, concentration of 1×10^4 colony forming units/mL) and *E.coli* suspension (1 mL, concentration of 1×10^4 colony forming units/ml) were inoculated into 6-well plates. After 24 h of incubation, the bacteria were subjected to different treatments. The cells were then stained with live and dead staining reagents (DAPI and PI probes) for 20 min before rinsing with phosphate buffer (PBS). Finally, images were recorded using an inverted fluorescence microscope[7, 9].

Determination of anti-biofilm mechanisms

Bacterial biofilm formation: *E.coli* and *S.aureus*, as common strains in infected wounds, were used to evaluate the biofilm resistance of the samples. *E.coli* (1×10^8 colony-forming units/mL, 1 mL) and *S.aureus* (1×10^8 colony-forming units/ml, 1 mL) were inoculated into 6-well plates with glass plates and incubated at 37℃ for 7 days to form mature biofilms. It is important to note that the medium was changed daily[3, 8].

Crystal violet (CV) staining of bacterial biofilms: CV staining was performed to visually visualize the biofilm. When a mature biofilm was formed, the sample was replaced into the medium containing the sample. After treatment, 200 μL of 2.5% glutaraldehyde solution was added to each well and the biofilm was fixed for 30 min. Next, biofilms were stained with 200 μL of 0.1% CV solution for 20 min. Finally, the stained biofilms were washed with phosphate buffer (PBS) and air-dried. To quantitatively measure the amount of residual biofilm, 200 μL of 33% acetic acid solution was added to each well to wash the stained biofilm. The absorbance (OD) value of each sample was measured at 570 nm[6].

Detection of reactive oxygen species (ROS) in bacteria: The content of ROS was detected by using the DCFH-DA probe. *S.aureus* suspension (1 mL, 1×10^4 colony-forming units/mL) and *E.coli* suspension (1 mL, 1×10^4 colony-forming units/ml) were respectively added to 6-well plates and cultured at 37℃ for 24 h. Subsequently, all the Wells were treated with different samples respectively. Then, under dark conditions, it was stained with a DCFH-DA probe at 37℃ for 15 min. Subsequently, all Wells were rinsed twice with phosphate buffered saline (PBS). Finally, the fluorescence images were captured using an inverted fluorescence microscope[7, 9].

Live-dead staining of bacterial biofilms: After biofilm formation, they were treated differently. Subsequently, live-dead staining was performed to detect the activity of bacteria in the biofilm. In brief, biofilms were covered with 200 μL of AO and PI probes and stained for 20 min. The cells were then washed three times with phosphate buffer (PBS). Images were taken using a confocal laser scanning microscope[10].

Assessment of cell viability *in vitro*: L929 mouse fibroblasts were used to evaluate the *in vitro* biocompatibility of the samples. L929 cells (1×10^4 cells/ml) were incubated with 1 ml of medium containing 89% DMEM medium, 10% fetal bovine serum and 1% antibiotics at 37℃ in a 5% CO_2 atmosphere.

MTT assay: L929 cells were seeded in 96-well plates and cultured for 12 h (5% CO_2, 37℃). 200 μL of sample solution with different concentration gradients were added to each well and incubated for 24 h. At the end of the incubation time, the medium was aspirated, and 20 μL of MTT solution (5 mg/mL) was added to each well and incubated for 4 h. Finally, all solutions were aspirated, 150 μL of DMSO was added, shaken, and the absorbance was measured using a microplate analyzer[9].

Live-dead staining assays of L929 cells: L929 cells (1×10^4 cells/ml) were seeded into 6-well plates and cultured for 24 h. After treatment of the cells with different samples, the cells were cultured for an additional 24 h and 48 h. For live or dead staining, the medium was removed, and 200 μL of calcein-AM and propidium iodine-PI probes were added to each well and incubated for 30 min at 37℃ At the end of the incubation period, the staining reagent was discarded and each well was washed twice with phosphate buffer (PBS). Images of stained cells were taken using a fluorescence microscope[11].

Cell scratch assay on L929 cells: L929 cells were seeded in 6-well plates and cultured using DMEM medium until confluence reached 90%-100%. Straight scratches were made perpendicular to the well plate with a 200 μL sterile gun tip or scratch device, and exfoliated cells were removed by gentle rinse with PBS. Scratch images were taken at 0 h under an inverted microscope. The cells treated with different samples were put back into the 37℃, 5% CO_2 incubator, and photographs were taken at 24 h and 48 h to record the scratch closure[11].

Blood compatibility testing

Hemolysis test: Hemolysis tests were performed to assess the blood compatibility of the samples. First, whole blood from mouse eyeballs was centrifuged at 3500 RPM for 5 min and washed several times with phosphate buffer solution (PBS). After that, 500 μL of the supernatant was mixed with different samples (at a concentration of 50 μg/mL in PBS) and incubated for 3 h at 37℃. Subsequently, the absorbance (OD) values of all sample supernatants were read at a wavelength of 545 nm. Water was used as a positive control group and PBS as a negative control group. The hemolysis rate for each sample was calculated using the following formula[11]:

$$\text{Hemolysis (\%)} = (OD_{sam}\text{-}OD_{neg}) / (OD_{neg}\text{-}OD_{pos}) \times 100\%$$

Among them, OD sample (OD_{sam}), OD negative (OD_{neg}), and OD positive (OD_{pos}) respectively represent the optical density of the sample, the negative control group, and the positive control group.

Evaluation of healing of infectious wounds *in vivo*

Construction of bacterial infection models: Healthy male Kunming mice (six-week-old males) were purchased from the Second Affiliated Hospital of Harbin

Medical University. Mice were randomly divided into four groups (n = 3): PBS group, POM group, D-POM group and L-POM group. All mice were anesthetized with 2% pentobarbital sodium (10 mL/kg), and the hair on their backs was shaved off for subsequent operations.

To establish a biofilm infection wound model, a full-thickness circular wound with a diameter of 10 mm was made on the back of each mouse. Add *S.aureus* (1×10^8 colony-forming units/ml, 10 μL) to the wound site, and then cover the wound with transparent sealing tape for 48 h. Two days later, a visible abscess formed at the wound site, and this day was designated as the first day. The wound images of the mice and the changes in their body weight were recorded on the 0th, 2nd, 4th, 6th, 8th and 10th days. On the 10th day, all mice were sacrificed and the tissues and organs (heart, liver, spleen, lungs, and kidneys) around the wounds were fixed with 4% paraformaldehyde for further histopathological analysis. Hematoxylin-eosin (H&E) staining was performed on all organs to evaluate the *in vivo* biocompatibility of the samples[11, 12].

Statistical Analysis

Quantitative experimental data were replicated three times. Statistical significance was assessed using Student's t-test when comparing two groups, and one-way analysis of variance (ANOVA) with SPSS software (version 27) was employed for comparisons involving more than two groups. All data were expressed as mean ± standard deviations (*$p < 0.05$, **$p < 0.01$, ***$p < 0.001$, $n = 3$). P values below 0.05 were considered statistically.

2. Supporting Figures

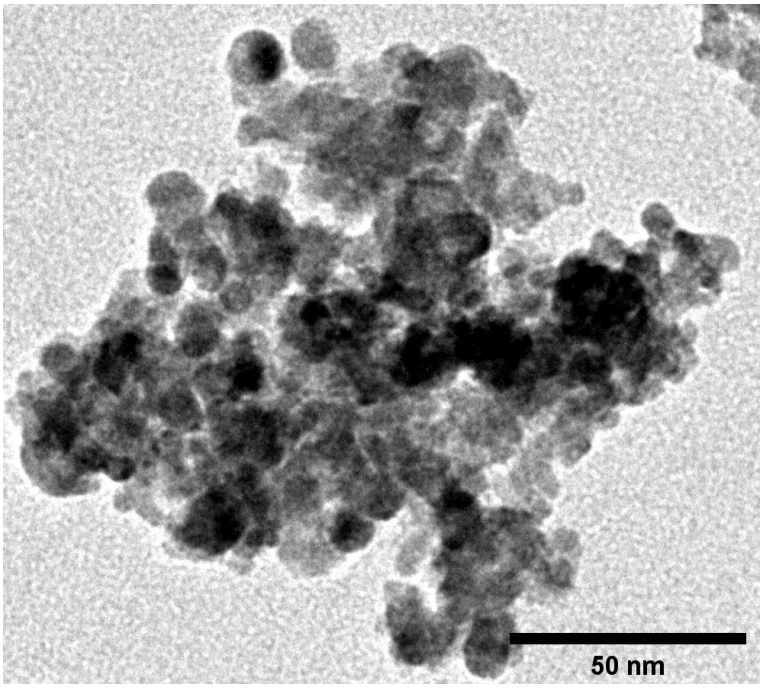

Figure S1. Transmission Electron Microscopy (TEM) image of POM.

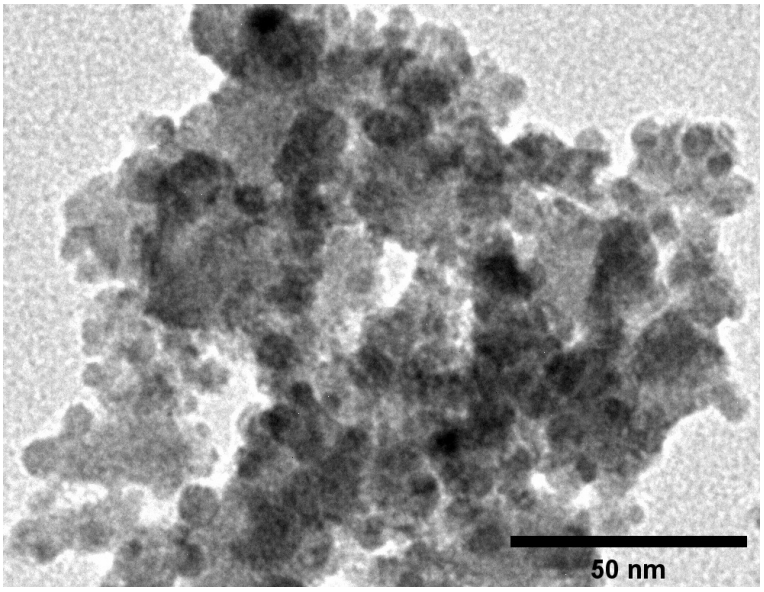

Figure S2. Transmission Electron Microscopy (TEM) image of D-POM.

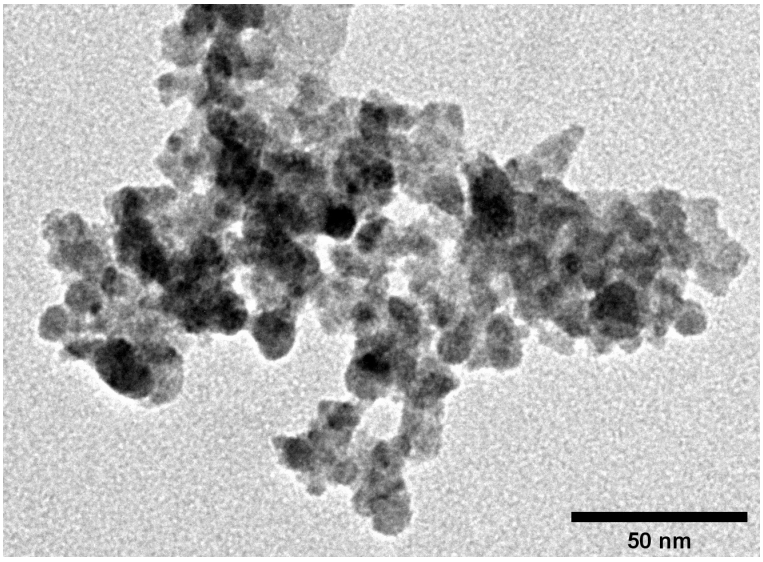

Figure S3. Transmission Electron Microscopy (TEM) image of L-POM.

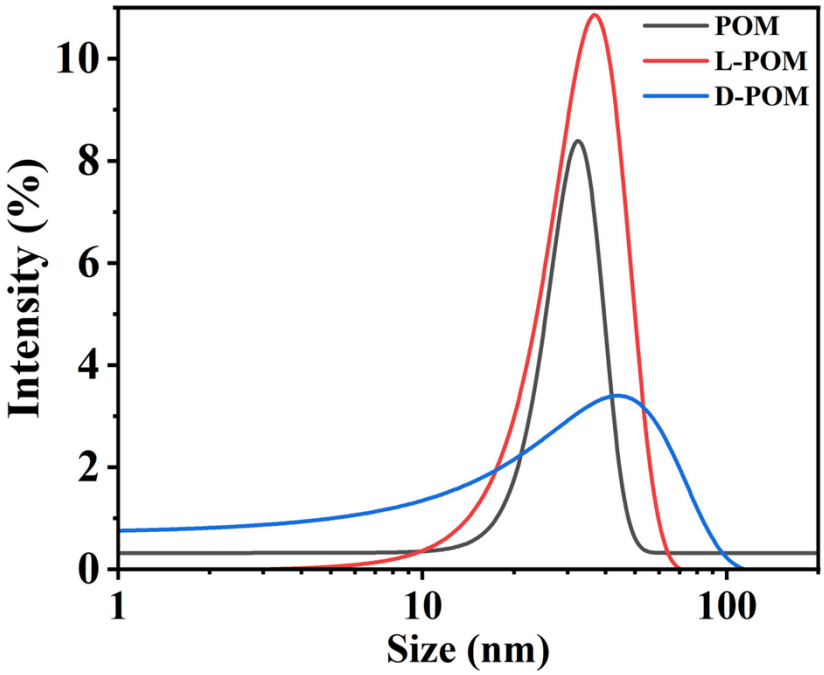

Figure S4. Hydrodynamic Size Distribution Analysis

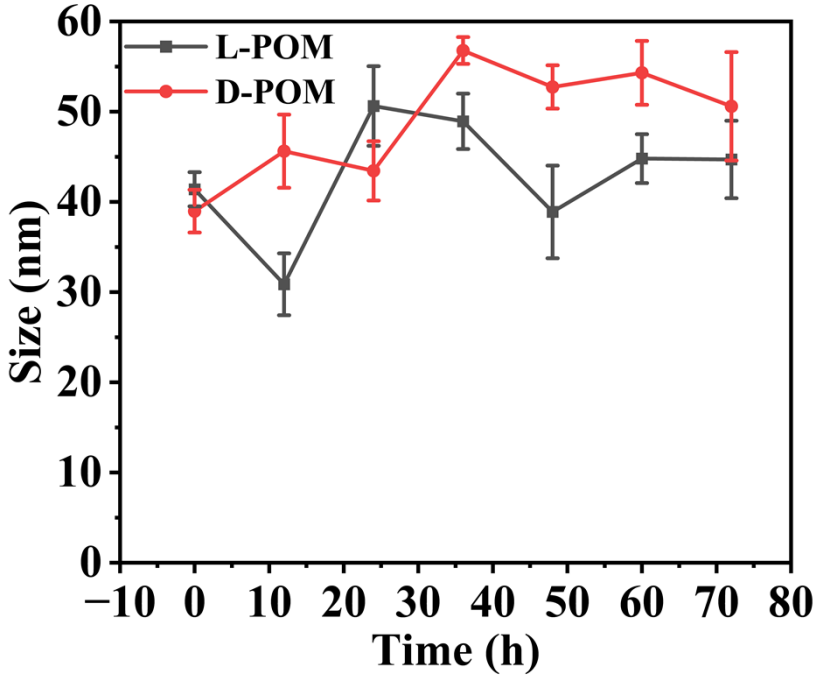

Figure S5. The DLS of D/L-POM in PBS.

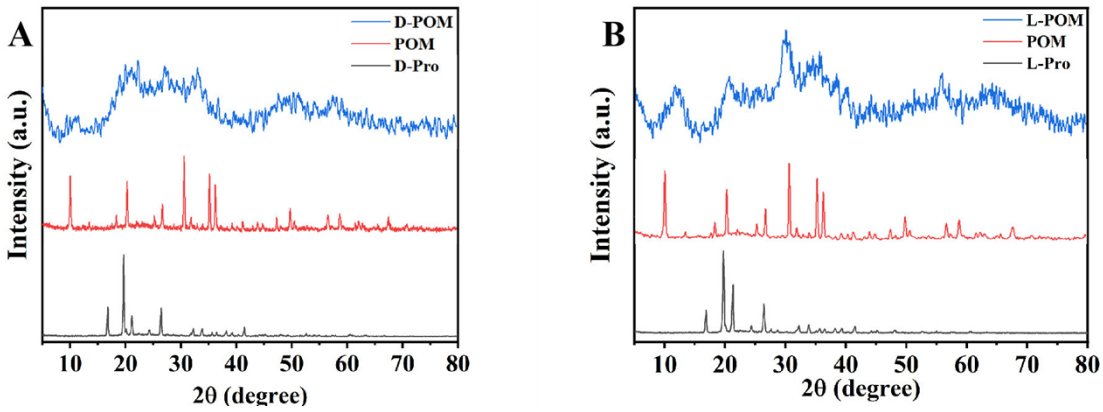

Figure S6. A) XRD spectrum of D-POM; B) XRD spectrum of L-POM.

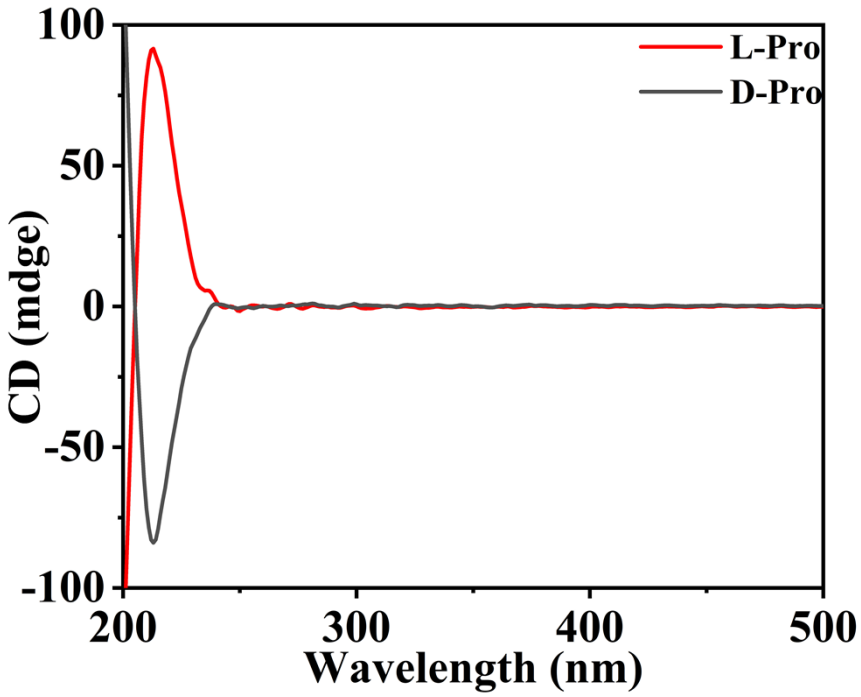

Figure S7. Chiral Circular Dichroism (CD) Spectra of D-Proline and L-Proline.

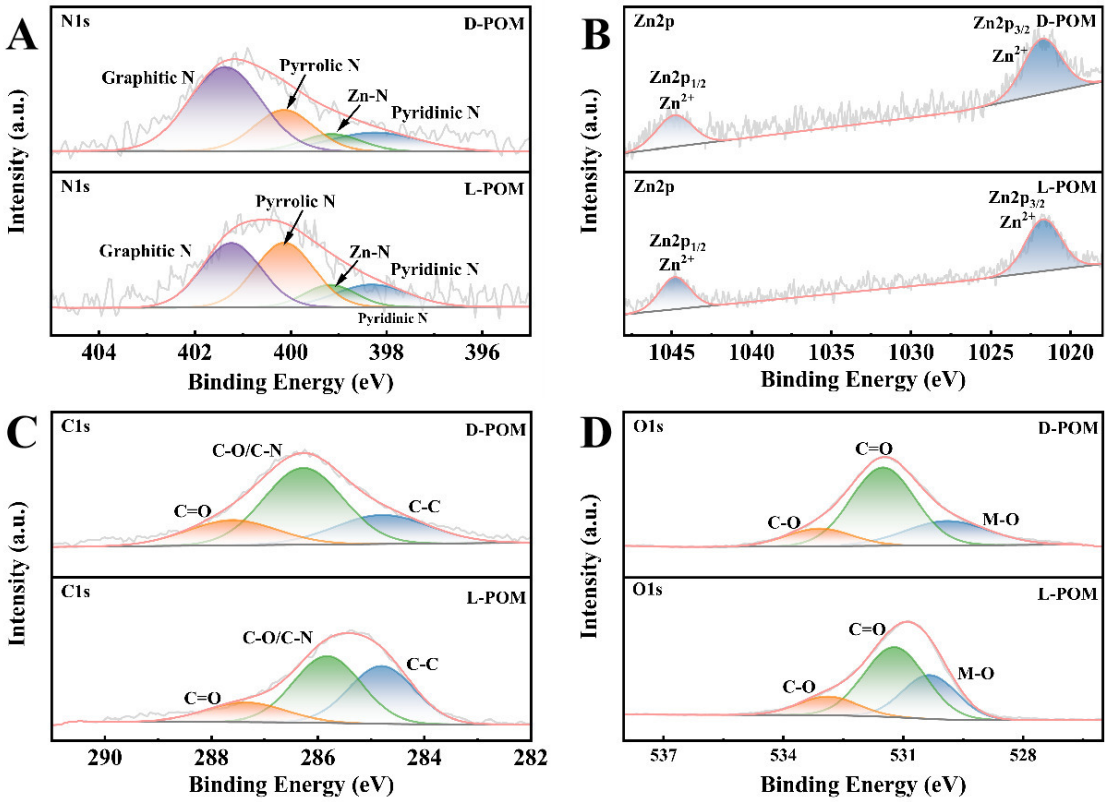

Figure S8. A) N1s spectra of D-POM and L-POM; B) Zn 2p spectra of D-POM and L-POM; C) C 1s spectra of D-POM and L-POM; D) O 1s spectra of D-POM and L-POM.

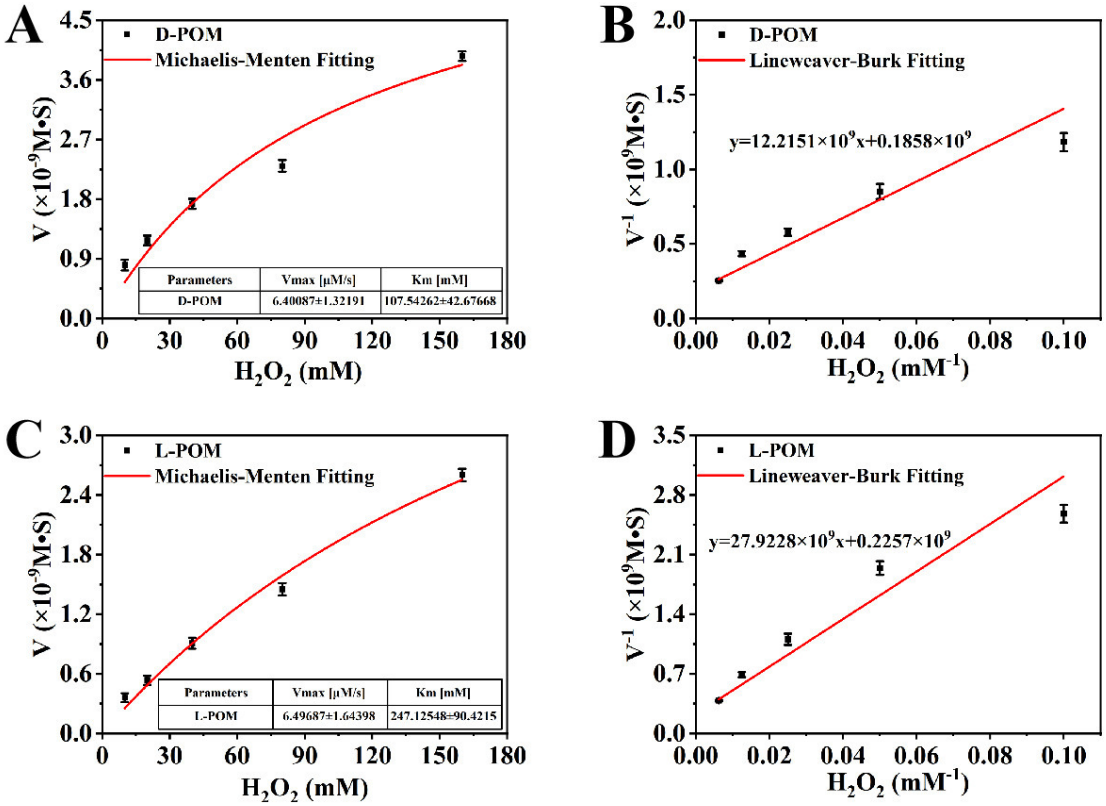

Figure S9. Analysis of Chemical Kinetic Performance: A) Michaelis-Menten kinetic curve of D-POM with H_2O_2 as substrate; B) Maximum reaction rate of D-POM with H_2O_2 as substrate; C) Michaelis-Menten kinetic curve of L-POM with H_2O_2 as substrate; D) Maximum reaction rate of L-POM with H_2O_2 as substrate. Data are expressed as mean ± standard error, n = 3.

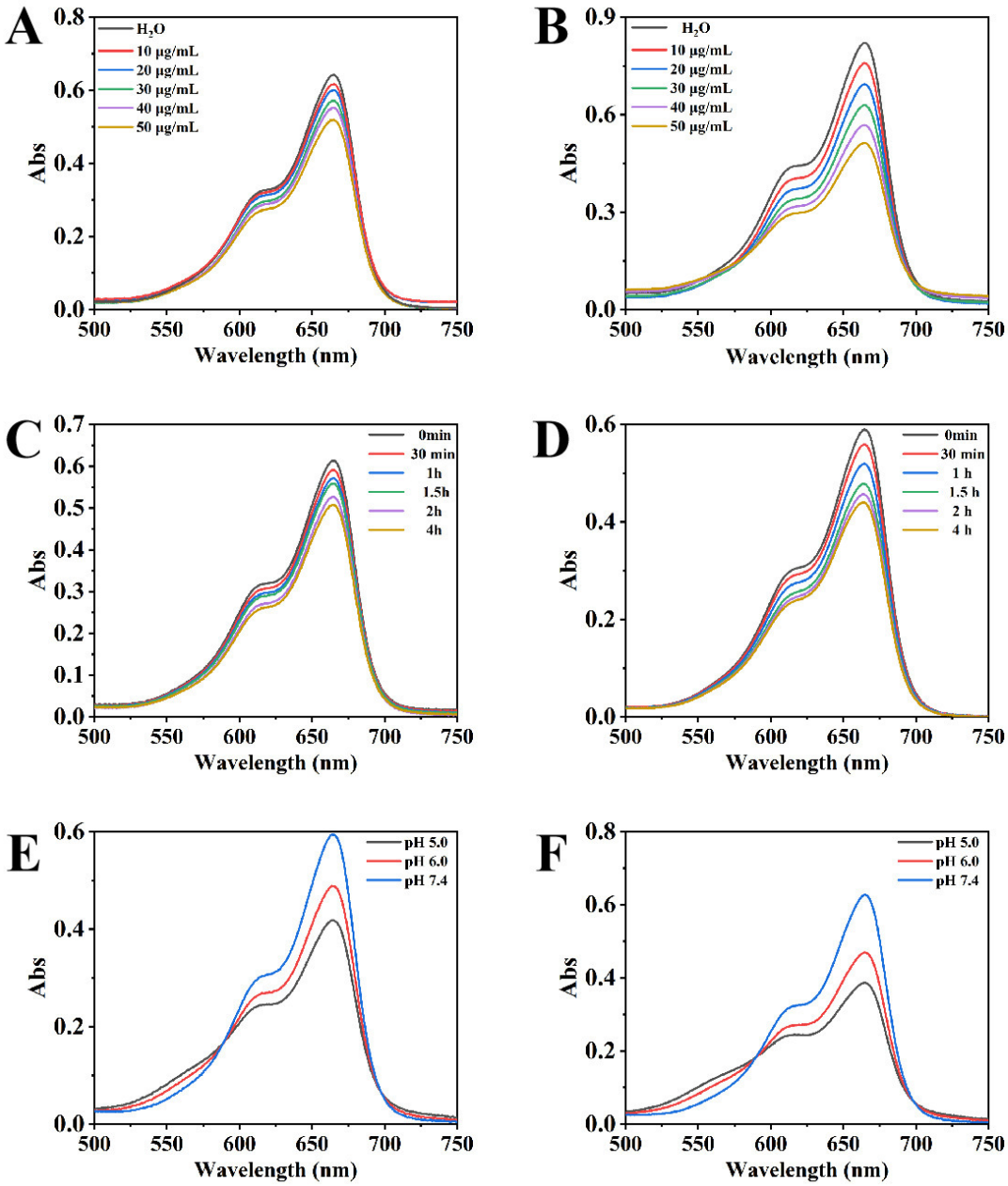

Figure S10. Catalytic performance analysis of D/L-POM: A-B) UV-Vis absorption spectra analysis of MB degradation catalyzed by D-POM and L-POM with varying concentrations of H_2O_2; C-D) UV-Vis absorption spectra analysis of MB degradation catalyzed by D-POM and L-POM over different time intervals; E-F) UV-Vis absorption spectra analysis of MB degradation catalyzed by D-POM and L-POM under varying pH conditions.

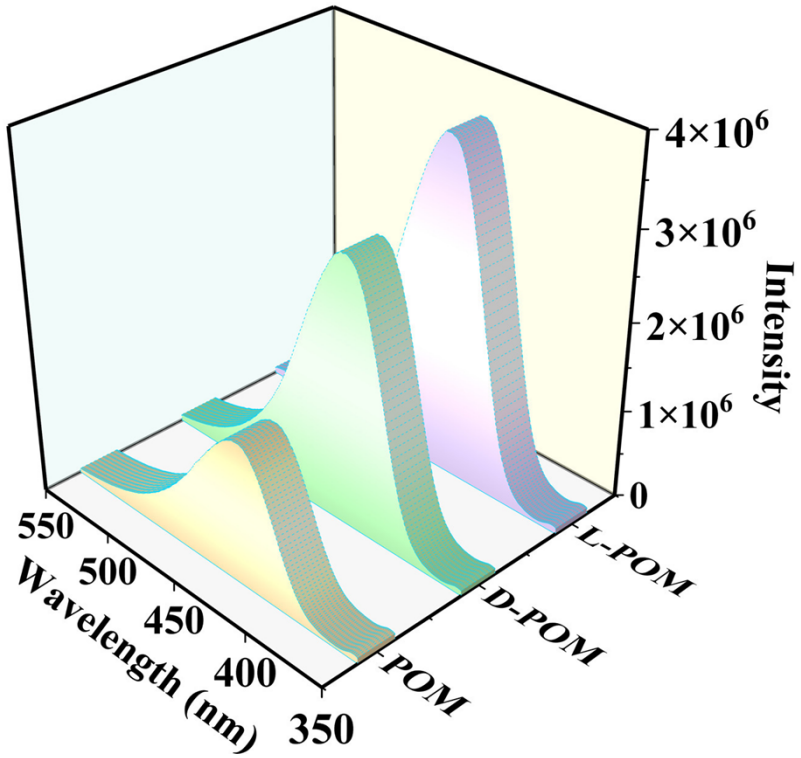

Figure S11. Fluorescence Spectroscopic Analysis of ·OH Generation from H_2O_2 Catalyzed by POM, D-POM, and L-POM (Using Terephthalic Acid as the Probe)

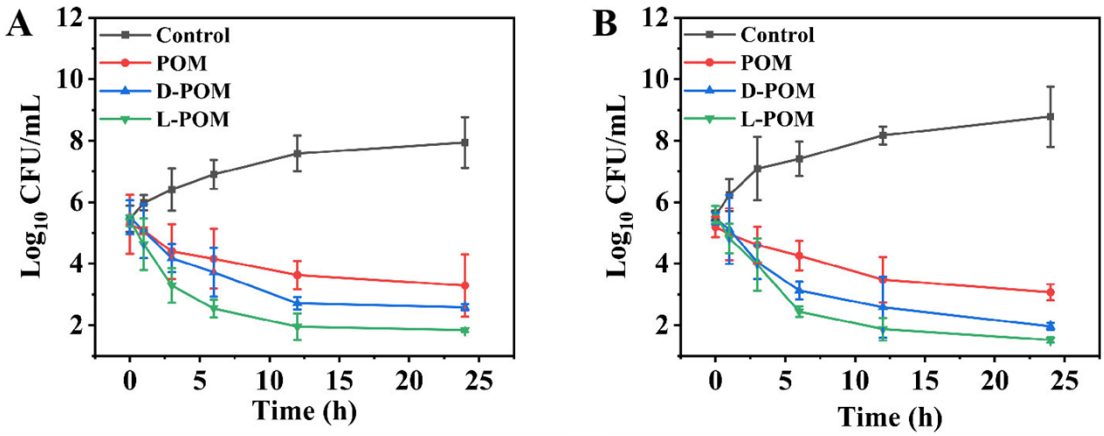

Figure S12. Time-kill curves *in vitro*: A) Time-kill curve of *E.coli* treated with different drugs; B) Time-kill curve of *S.aureus* treated with different drugs. Data are expressed as mean ± standard error, n = 3.

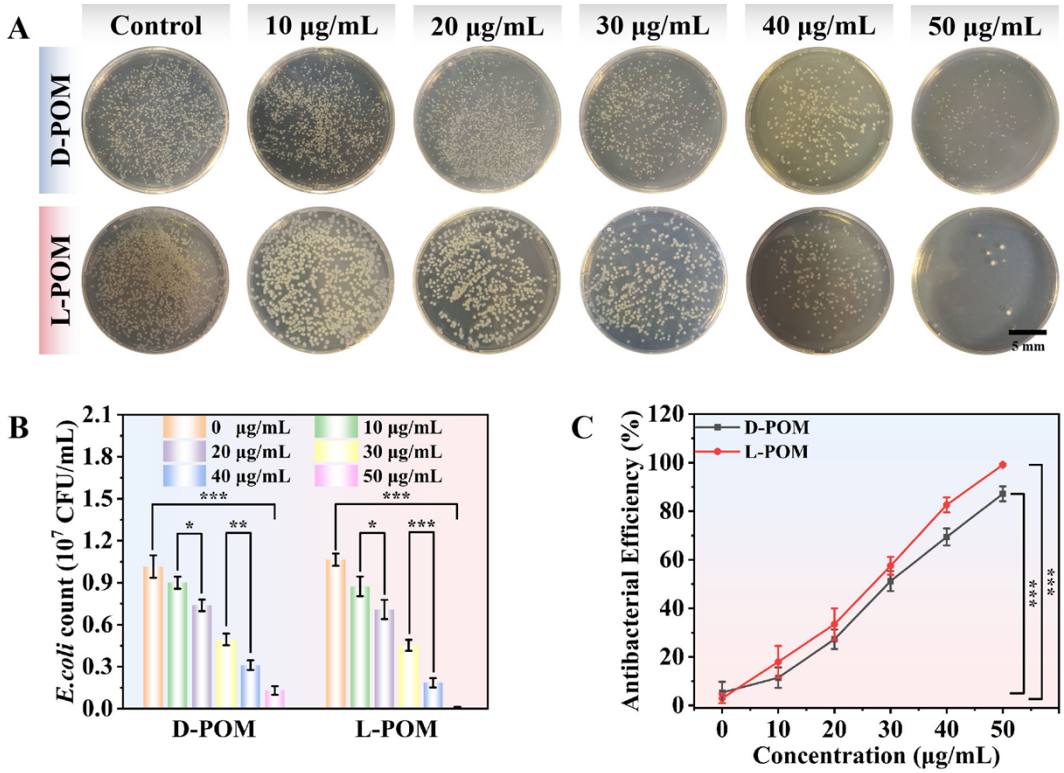

Figure S13. *In Vitro* Antibacterial Assay of *E.coli*: A) Optical images of *E.coli* treated with varying concentrations of D-POM and L-POM; B) Enumeration of *E.coli* as depicted in (A); C) Antibacterial rate of *E.coli* as illustrated in (A). Data are expressed as mean ± standard error, n = 3. $p < 0.05$ (*), $p < 0.01$ (**), and $p < 0.001$ (***).

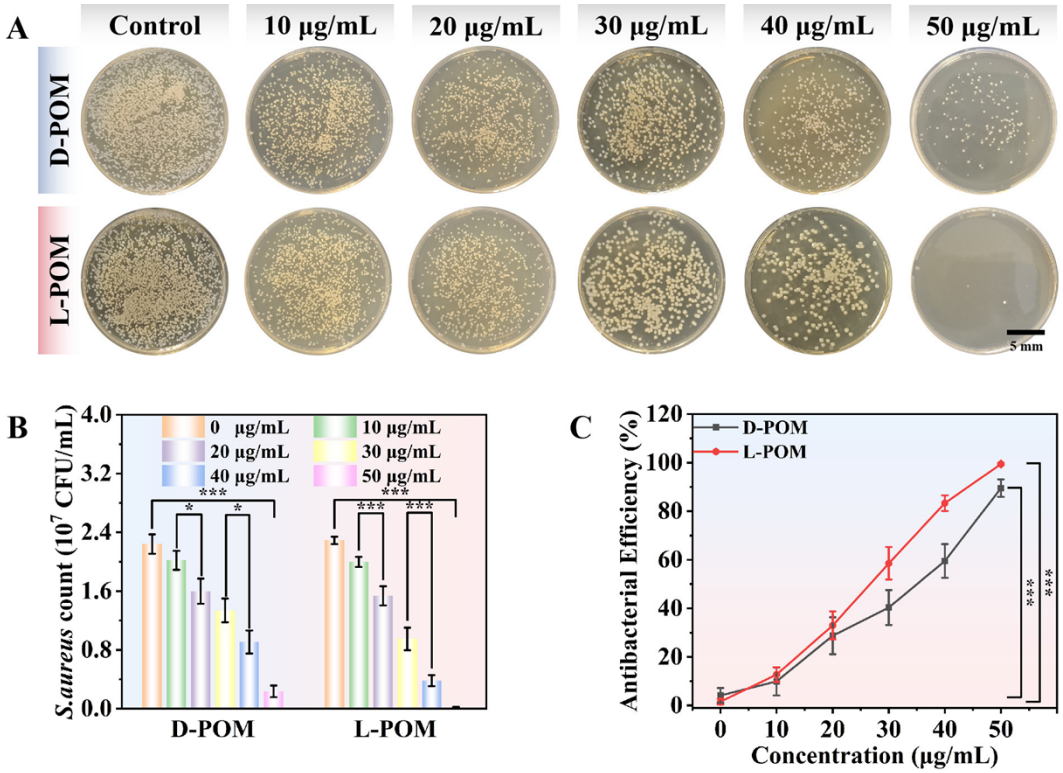

Figure S14. *In Vitro* Antibacterial Assay of *S.aureus*: A) Optical images of *S.aureus* treated with varying concentrations of D-POM and L-POM; B) Enumeration of *S.aureus* as depicted in (A); C) Antibacterial rate of *S.aureus* as illustrated in (A). Data are expressed as mean ± standard error, n = 3. $p < 0.05$ (*), $p < 0.01$ (**), and $p < 0.001$ (***).

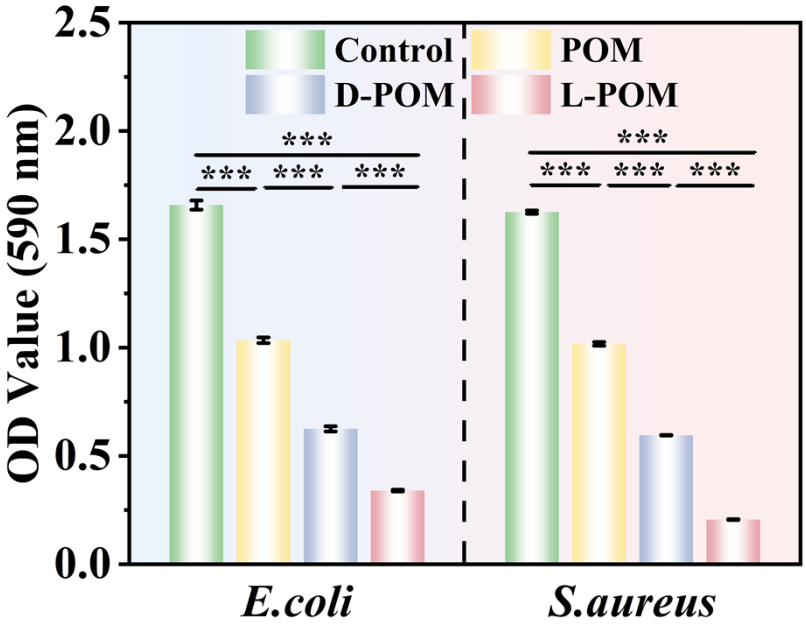

Figure S15. UV-Vis absorption spectra of crystal violet assay for bacterial biofilm formation. Data are expressed as mean ± standard error, n = 3. $p < 0.05$ (*), $p < 0.01$ (**), and $p < 0.001$ (***).

References

1. Y. Song, Y. Sun, M. Tang, Z. Yue, J. Ni, J. Zhao, W. Wang, T. Sun, L. Shi and L. Wang, *ACS Applied Materials & Interfaces*, 2022, **14**, 4914-4920.
2. H. Y. An, E. B. Wang, D. R. Xiao, Y. G. Li, Z. M. Su and L. Xu, *Angewandte Chemie International Edition*, 2006, **45**, 904-908.
3. C. Geng, S. He, S. Yu, H. M. Johnson, H. Shi, Y. Chen, Y. K. Chan, W. He, M. Qin, X. Li and Y. Deng, *Advanced Materials*, 2024, **36**, e2310599.
4. J. W. Dong, S. T. Zhang, Y. K. Chan, S. Q. Lai and Y. Deng, *Biomaterials*, 2025, **320**, 123258.
5. Q. Y. Meng, W. X. Wang, H. Z. Wang, Y. Tao, N. Anastassova, T. D. Sun, Y. Sun and L. Wang, *Journal of Colloid and Interface Science*, 2025, **678**, 796-803.
6. Y. Huang, J. Li, Z. Yu, J. Li, K. Liang and Y. Deng, *Advanced Materials*, 2024, **36**, 2414111.
7. H. Z. Wang, D. Li, Q. Y. Meng, X. Li, K. L. Guo, Z. H. Zou, J. S. Peng, Y. Sun and T. D. Sun, *Macromolecular Rapid Communications*, 2024, **45**, 2400415.
8. J. Gong, S. Q. Lai, S. T. Zhang, K. N. Liang and Y. Deng, *Small*, 2025, **21**, 2409437.
9. M. L. Tang, J. T. Ni, Z. Y. Yue, T. D. Sun, C. X. Chen, X. Ma and L. Wang, *Angewandte Chemie International Edition*, 2024, **63**, e202315031.
10. J. Yang, K. Liu, Y. Chen, H. Ye, G. Hao, F. Du and P. Wang, *Nature Communications*, 2025, **16**, 2627.
11. L. L. Zong, R. X. Teng, H. Q. Zhang, W. S. Liu, Y. Feng, Z. M. Lu, Y. X. Zhou, Z. Fan, M. Li and X. H. Pu, *Advanced Science*, 2024, **11**, 2406022.

12. M. M. He, Z. Y. Wang, D. N. Xiang, D. Sun, Y. K. Chan, H. L. Ren, Z. J. Lin, G. F. Yin, Y. Deng and W. Z. Yang, *Advanced Materials*, 2024, **36**, e2405659.